Jordan Journal of Civil Engineering, Volume **5**, No. **1**, **2011**

Modeling of the Behavior of Expansive Soils

***Aissa Mamoune, S.M.*[1)] *and Bekkouche, A.*[2)]**

[1)], [2)] Department of Civil Engineering, Faculty of Technology, University of Aboubakr Belkaïd-Tlemcen, Po. Box 230, Tlemcen (13000), Algeria. E-Mail: sm_aissa@mail.univ-tlemcen.dz
a_bekkouche@mail.univ-tlemcen.dz

ABSTRACT

In the preliminary reconnaissance phase and once the swelling of soil is suspected, it is possible to obtain an estimation of swelling parameters (amplitude and pressure) using numerous rheological models proposed in the literature. These models relate the parameters of swelling to the geotechnical parameters determined from mechanical tests. The analysis of the behavior of clays is conducted by numerical simulation tests of compression and swelling by using the oedometer. This analysis is conducted using the software CASTEM2000 team from CEA-France. This simulation allows-among others-to develop a predictive procedure for estimating the parameters of swelling by the use of constitutive equations of Cam-Clay and Alonso. It should be noted that different simulations are performed; those using oedometer tests by the Cam-Clay model, and Alonso and free swell tests by the Alonso model. The results of this work show that the compressibility has been correctly simulated by both models. The phase of swelling has been simulated by the model of Alonso as the Cam-Clay model can simulate it. It should be noted that the Alonso model underestimates very fluffy swelling soils.

KEYWORDS: Swelling clay, Numerical modeling, Behavior, Cam-Clay, Alonso.

INTRODUCTION

To model the behavior of clays, it seems necessary to move towards elastoplastic laws having been used for different types of clays. There are several models describing with more or less success the elastoplastic mechanical behavior of clays normally consolidated or overconsolidated. These include the rheological models, Cambridge: original and modified Cam-Clay (1968) and more recent models, such as Lade (1977), Norris and Zienkewich (1979), Hujeux (1985), Nova and Heuckel (1980), Mroz (1980), Alonso (1990), Abu Bakr (1995) and Pakzad (1995), which have been developed to improve the prediction of the behavior of clays.

Accepted for Publication on 15/1/2011.

Despite their simplicity, models of Cambridge seem to describe the behavior of normally consolidated and slightly overconsolidated clays, whereas the Hujeux model is suitable for overconsolidated clays (Pakzad, 1995).

In this work, a simulation of the mechanical behavior of clays will be attempted using the Cam-Clay model and Alonso model.

Cam-Clay Models

The first models for strain hardening elastoplastic soils have been developed by a team from the University of Cambridge. Thus, Roscoe, Schofield and Wroth Poorooshash (1958-1968) developed the first version of the Cam-Clay models. Burland (1965-1967) changed this version.

Original Cam-Clay

The original model was developed from the plastic work expression:

$$dW^p = P'.d\varepsilon_v^p + q.d\varepsilon_d^p$$

Where P' and q represent the deviatoric and volumetric parts of the tensor of effective stresses. ε_v and ε_d represent the deviatoric and volumetric strain:

$$P = \frac{1}{3} I_1 = \frac{1}{3} \sum \sigma_{ii}$$

$$q = \left(\frac{3}{2} s_{ij} . s_{ij} \right)^{\frac{1}{2}}$$

where $s_{ii} = \sigma_{ii} - P.\delta_{ii}$

$$\varepsilon_v = \sum \varepsilon_{ii}$$

$$\varepsilon_d = \left(\frac{2}{3} e_{ij} . e_{ij} \right)^{\frac{1}{2}}$$

$$e_{ij} = \varepsilon_{ij} - \frac{\varepsilon_v}{3}$$

In the case of axisymmetric, triaxial and oedometer tests ($\sigma_2 = \sigma_3$), these invariants follow the following expressions:

$$P = \frac{1}{3} \left(\sigma_1 + \sigma_2 + \sigma_3 \right)$$

$$q = \sigma_1 - \sigma_3$$

$$\varepsilon_v = \varepsilon_1 + \varepsilon_2 + \varepsilon_3$$

$$\varepsilon_d = \frac{2}{3} \left(\varepsilon_1 - \varepsilon_3 \right)$$

Modified Cam-Clay Model

This model differs from the original model by stating the plastic energy which involves a volume contribution (Callari et al., 1998):

$$DW^P = \sqrt{(P'.d\varepsilon_v^p)^2 + (q.d\varepsilon_d^p)^2} \ .$$

The trace of the threshold in (p', q) becomes ellipsoidal while maintaining the same level for the critical state and eliminating the vicinity of q = 0, the conical point that presents the original model. The charging function is defined by:

$$F = q^2 + M^2 P' \left(P' - 2Pc \right) = 0$$

$$P_{co} = \frac{P_0}{2} \ .$$

The flow rule according to the equations is as follows:

$$\frac{d\varepsilon_v^p}{d\varepsilon_d^p} = \frac{\left(M^2 - \frac{q^2}{P'^2} \right) P''}{2q} \ .$$

The schematization of the two Cam-Clay load surfaces, (Original and modified), is presented in Figure 1.

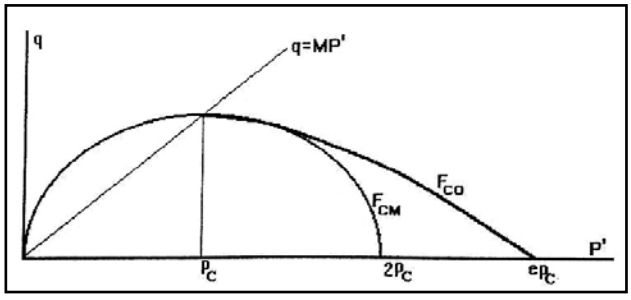

Figure 1: Simulation of load surface, F_{CO} : the original Cam-Clay surface, F_{CM} : modified Cam-Clay surface (Pakzad, 1995)

Alonso Model

The model is developed by the team of Barcelona: Alonso, Gens and Josa on the basis of the modified Cam-Clay model (Alonso et al., 1990). It considers that the suction is an independent variable, $s = u_a - u_w$. The model is formulated based on the following assumptions:

H1: The increase in elastic limit (or preconsolidation stress) with negative pressure.

H2: The suction decreases the compressibility of the soil and increases the mechanical strength of the soil under an external constraint.

H3: During a cycle drainage humidification, reversible volumetric strains are produced.

H4: At given constraints, the reduction of suction (wetting) may induce irreversible volumetric deformation (collapse).

H5: When the confining stress increases, the magnitude of the collapse increases to a maximum value, then it decreases.

H6: The saturation of the material leads it to join the initial stress-strain path in the saturated state.

H7: The path to a constant suction is an independent path.

H8: Increasing the suction causes the growth of capillary cohesion.

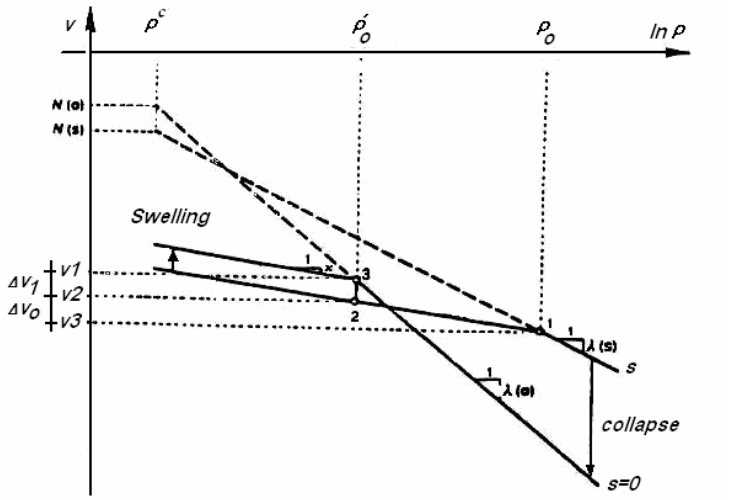

Figure 2: Schematic representation of compressibility slopes, preconsolidation pressure for a saturated soil and unsaturated soil in a compression-decompression path

Changes in Volume As a Result of Isotropic Stress

The determination of load surfaces in (*P, s*) is based on the fact that suction decreases the compressibility of the soil. *P* is considered a crude average pressure ($P = p - u_a$). The consolidation conditions to a given suction, can be idealized by two straight lines characterized by two slopes defined by *k* for the overconsolidated part (the elastic slope) and *λ(s)* for the normally consolidated part (elasto-plastic part) in the plane (*v*, *Ln P*) as shown in Figure 2. *k* is assumed to be independent of suction and λ(s) varies with suction as follows:

$$\lambda(s) = \lambda(0) \cdot \left[(1-t) \cdot \exp(-\zeta . s) + t\right]$$

where:

λ(s): the slope of compressibility in the saturated state,

t: a constant related to maximum stiffness when the soil suction tends to infinity,

ζ: a constant that controls the rate of increase in stiffness with suction.

The specific volume of soil in the normally consolidated state is given by the following equation:

$$v = 1 + e = N(s) - \lambda(s).Ln\frac{P}{P^0}$$

where P^0 is a reference strain for $v = N(s)$.

The behavior of the soil during the unloading-reloading cycle is elastic, and swelling due to mechanical unloading is expressed by:

$$dv = -k\frac{dP}{P}$$

The swelling due to wetting is expressed by:

$$dv_s = -k_s\frac{ds}{s + P_{at}}$$

where:

k_s: the compressibility factor corresponding to the change of suction in the elastic region,

P_{at}: atmospheric pressure.

From these assumptions, Alonso et al. obtained an equation expressing the relationship between P_{c0}, the preconsolidation pressure in the saturated state, and $P_{c0}(s)$, the apparent preconsolidation pressure at a given suction, which is as follows:

$$\frac{P_{C0}(s)}{P^0} = \left(\frac{P_{C0}}{P^0}\right)^{[\lambda(0)-k]/[\lambda(s)-k]}$$

With this equation, the appearance of strain hardening of unsaturated soils can be described with one parameter of strain hardening P_{C0}. This equation defines, in fact, in *(P, s)* a curve called LC (Loading Collapse) which separates the elastic region to the left from the elasto-plastic region to the right. If $P_{C0} = P^0$, the LC curve becomes a straight line, and in this case the change of *s* produces no plastic deformation (Alonso et al., 1999). Only the elastic deformation occurs.

The increased suction can cause irreversible deformations. It is proposed that the soil approaches a maximum value s_0. With the lack of experimental results, the authors propose a limit and a simple expression: $s = s_0$ = constant.

s_0 is the maximum suction suffered by the soil in its history and is taken as a parameter of strain hardening in suction. Thus, the elastic zone is well defined by the LC curve and the line $s = s_0$ named SI (Suction Increase) (see Figures 3 and 4).

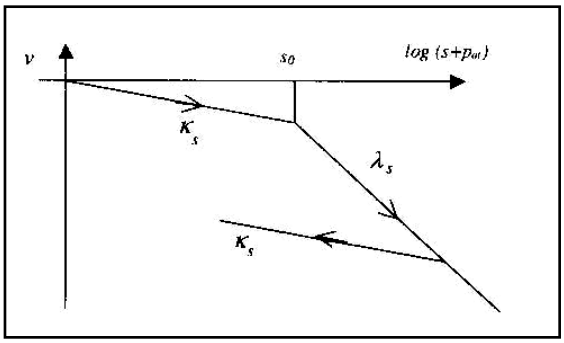

Figure 3: Definition of the elastic limit of suction s_0 in the *(s - v)* plane

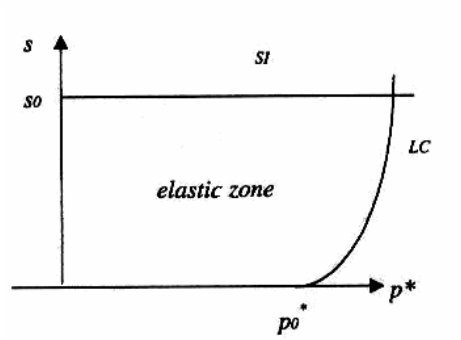

Figure 4: The elastic zone and the position of SC and SI curves in the plane *(P, s)*

With the linear relationship between *v* and *Ln* ($s + P_{at}$) in the two parts; elastic and elastoplastic, we can write:

$$dv_s = -\lambda_s\frac{ds}{s + P_{at}}$$

For the reversible wetting and drainage, we have:

$$dv_s = -k_s\frac{ds}{s + P_{at}}$$

Hardening Law and Coupling between SL and LC

The increase of *P* in the elastic deformation induced by volume compression (positive) is given by:

$$d\varepsilon_v^e(p) = -\frac{dv}{v} = \frac{k}{v}\frac{dP}{P}.$$

When the average pressure P passes the crude pressure P_{C0} (s), the compressibility can be calculated by the following equation:

$$d\varepsilon_v(p) = \frac{\lambda_1(s)}{v}\frac{dP_{C0}(s)}{P_{C0}(s)}$$

At constant suction, the plastic volumetric strain is calculated by the equation:

$$d\varepsilon_v^p(p) = \frac{\lambda_1(s)-1}{v}\frac{dP_{C0}(s)}{P_{C0}(s)}$$

The strain at the saturated state is given as:

$$d\varepsilon_v^p(p) = \frac{\lambda_1(0)-1}{v}\frac{dP_{C0}(s)}{P_{C0}(s)}$$

Similarly, for the volumetric strain due to the variation of suction, we have:

$$d\varepsilon_v^e(s) = \frac{k_s}{v}\frac{ds}{(s+P_{at})}$$

$$d\varepsilon_v(s) = \frac{\lambda_s}{v}\frac{ds_0}{(s_0+P_{at})}$$

$$d\varepsilon_v^P(s) = \frac{\lambda_s - k_s}{v}\frac{ds_0}{(s_0+P_{at})}$$

where s is the coefficient of compressibility in the zone $s > s_0$.

The irreversible deformation controls the position of SC and SI zones. This type of hardening defines the movement of SI and SC independently (Figure 5).

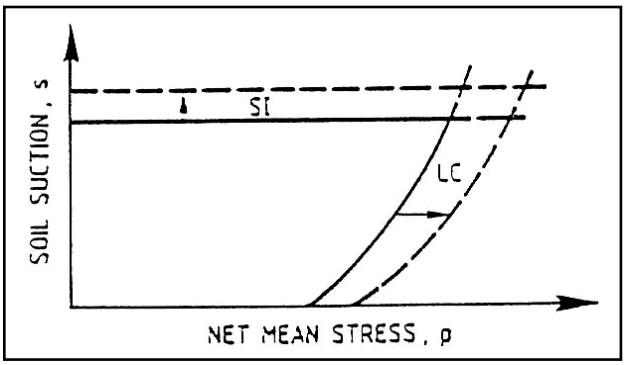

Figure 5: The movement of surfaces SC and SI because of plastic deformation

To introduce the coupling effect, Alonso et al. took the total plastic deformation:

$$d\varepsilon_v^p = d\varepsilon_v^p(s) + d\varepsilon_v^p(p)$$

Thus, the hardening is given by:

$$\frac{dP_{C0}}{P_{C0}} = \frac{v}{\lambda_1(0)-k}d\varepsilon_v^p$$

So, a shift of SI causing irreversible deformation $d\varepsilon_v^p(s)$ moves the LC curve to the right and *vice versa*.

Extension of Deviatoric Stress State Model

It should be noted that from the aspect of deviatoric observation concerning the effect of suction, cohesion is to increase with suction. That is why the authors made the following assumptions:

H1: The suction increases cohesion linearly while maintaining the slope of the projection of the critical state curve M constant. The ellipse of the loading surface and the curve M intersects with the mean stress axis in abscissa:

$$P = -P_s = -k_s$$

where k is a constant (Figure 6-a).

Assuming that the load surface in the *(P-q)* plane at a given suction is elliptical, we can write the equation of this surface as:

$$F(s) - q^2 + M^2(P+P_s)(P-P_{C0}(s)) = 0$$

The three-dimensional view of surfaces in the space *(P, q, s)* is shown in Figure 6-b.

H2: The flow rule is non-associated using a coefficient γ to allow having a good agreement with the experimental value K_0 which is often overestimated.

$$\frac{d\varepsilon_d^p}{d\varepsilon_v^p(p)} = \frac{2q\gamma}{M^2(2P+P_s-P_0)}$$

where γ can be determined by the condition with K_0 (oedometer test):

$$K_0 = 1-\sin\phi' = (6-2M)/(6+M)$$

$$\gamma = \frac{M(M-9)(M-3)}{9(6-M)}\frac{\lambda(0)}{\lambda(0)-k}$$

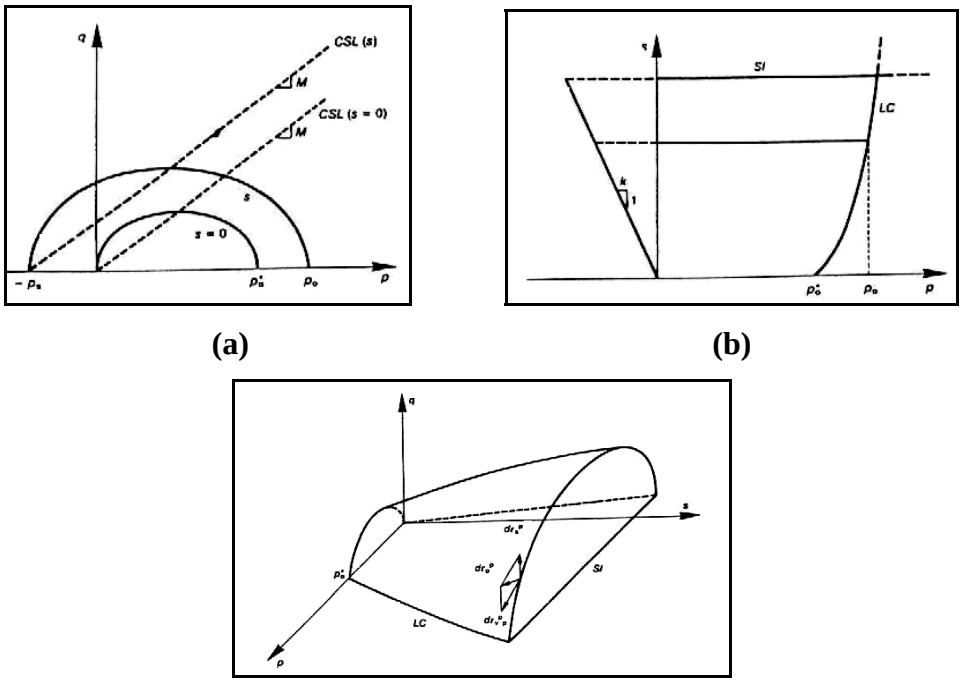

Figure 6: Representation of loading surface in the space *(P, q, s)*

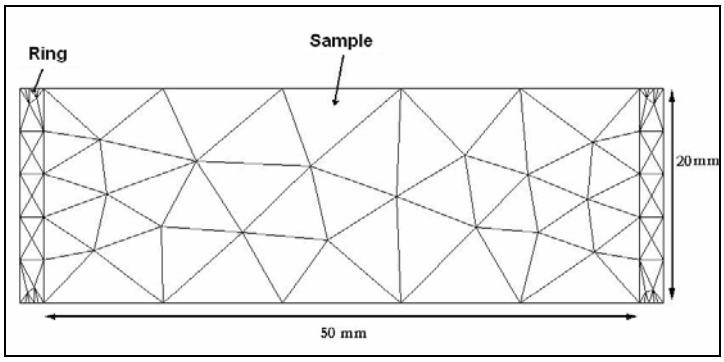

Figure 7: Mesh sample

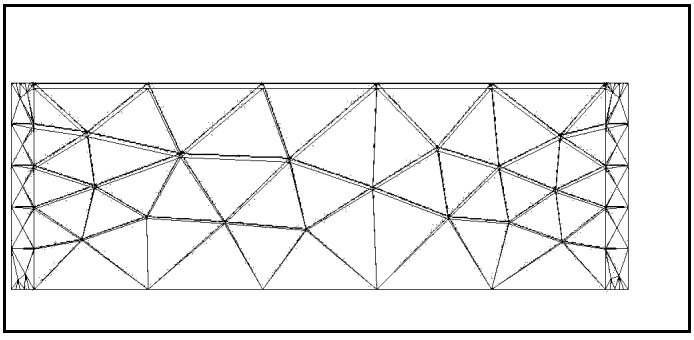

Figure 8: Deformed shape

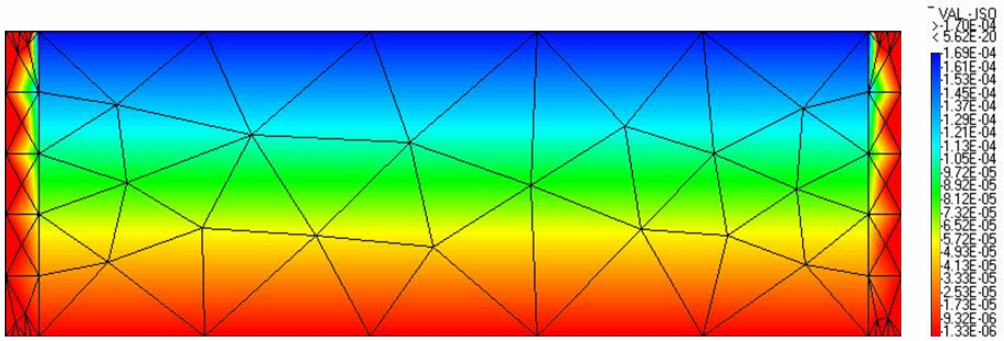

Figure 9: Variation of the deformation within the sample

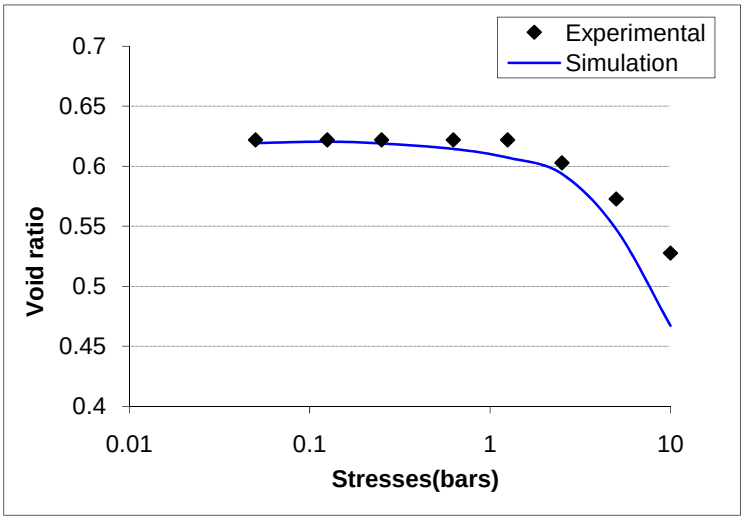

(a): Site of Ouled Mimoun, Pc_0 = 2.4 bar e_0 = 0.6219

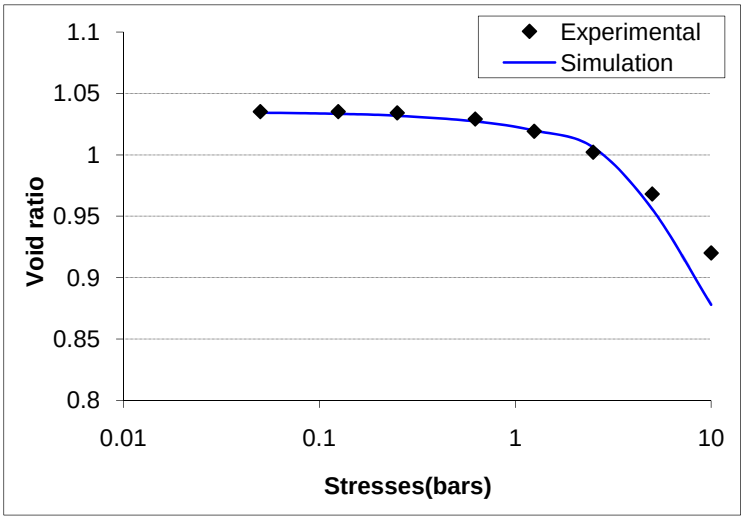

(b) : Site of Bab El Assa, Pc0 = 2.5 bar, e_0 = 1.035

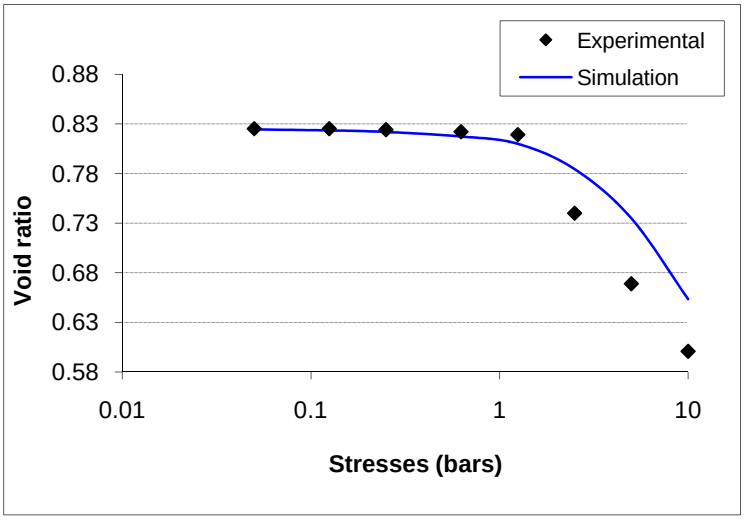

(c): Site of Bab El Assa Pc0 = 1.4 bar, e_0 = 0.825

Figure 10: Simulation of oedometer tests by the Cam-Clay model

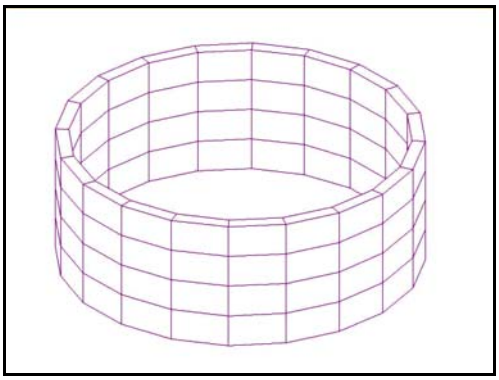

Figure 11: The mesh of the ring

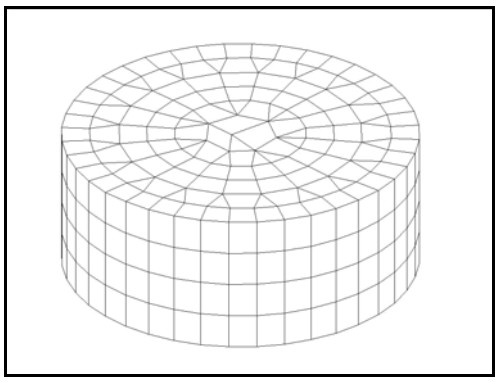

Figure 12: The mesh of the sample

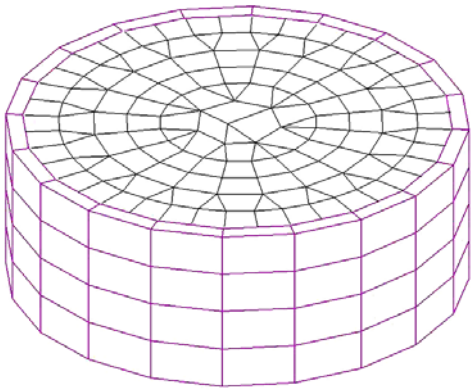

Figure 13: The mesh of the sample and the ring

H3: For elastic shear deformation, the following classical equation has been taken:

$$d\varepsilon_d^e = \frac{dq}{3G}.$$

Simulation of Oedometeric Tests by Cam-Clay Model

A numerical simulation of oedometric tests is conducted using the Cam-Clay model through the Castem 2000 software. This simulation is performed on samples from the sites Ouled Mimoun and Bab El Assa, for which oedometric tests were performed.

Figure 7 shows the mesh and dimensions of the sample with the ring used in the simulation. The soil sample has a diameter of 50 mm and a height of 20 mm, while the ring has a thickness of 2 mm. A finite element mesh using triangular elements with three nodes was established. For better simulating the oedometric test, we considered the effect of friction between the sample and the ring by defining a frictional force in the contact area.

Several simulations were carried out to test the reliability of the model. The deformed shape (Figure 8) and the deformation within the sample (Figure 9) were calculated. From this last figure, the void ratio is obtained which is associated with the level of loading. Finally, to draw the oedometric curve of a sample and then simulate the oedometric test, the load is varied to obtain the void ratio associated with different stresses.

This methodology is applied to samples from different sites (Ouled Mimoun and Bab El Assa). The results obtained by the model show very good convergence of experimental and theoretical values. Indeed, the error rate obtained for these simulations rarely exceeds 9% (Figure 10).

However, the major disadvantage of this model is that it does not simulate the unloading phase of an oedometer test, because once the loading surface is achieved after one level of loading, the material returned to plasticity. Thus, the unloading is done under an elastic behavior, which is not consistent with the reality of material behavior. Therefore, a simulation of the oedometer tests by Alonso model, described above, is necessary.

Simulation of Oedometric Tests by Alonso Model

This section is devoted to the simulation of the oedometer tests by the Alonso model. The dimensions of the sample and the ring are the same as those used for the previous model. For this simulation, we opted for a finite element mesh using 8-node cubic elements. Figures 11, 12 and 13 represent respectively the mesh of the ring, the mesh of the sample and the mesh of the sample and the ring.

To compare simulation results with those previously obtained, the same samples were used. The latter model shows a marked decrease in the error between experimental and theoretical results. Indeed, the error rate obtained for the latter model rarely exceeds 6% (Figure 14).

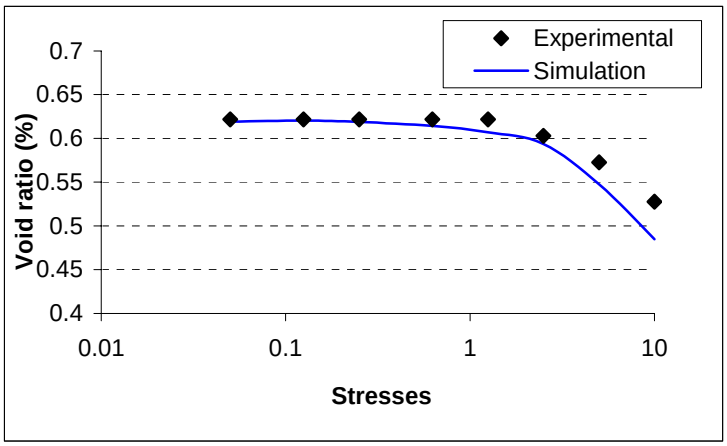

(a): Site of Ouled Mimoun, Pc_0 = 2.4 bar e_0 = 0.6219

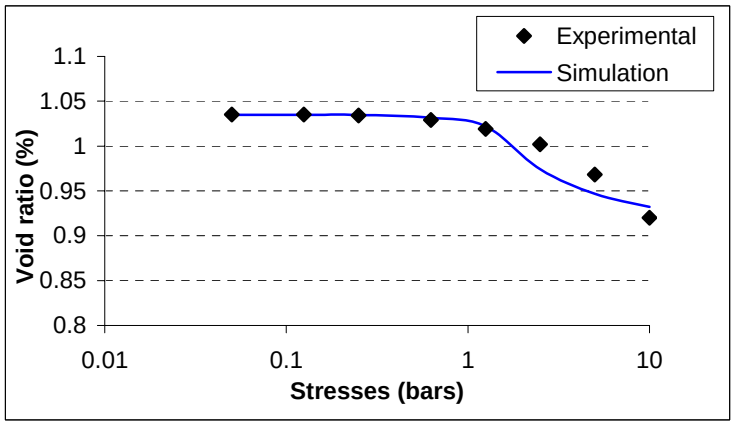

(b): Site of Bab El Assa, Pc_0 = 2.5 bar, e_0 = 1.035

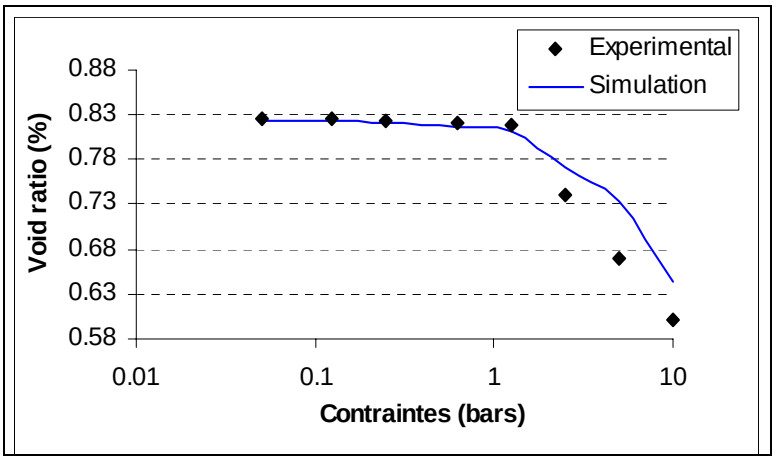

(c): Siteof Bab El Assa, Pc_0 = 1.4 bar, e_0 = 0.825

Figure 14: Simulation of oedometric tests by the Alonso model

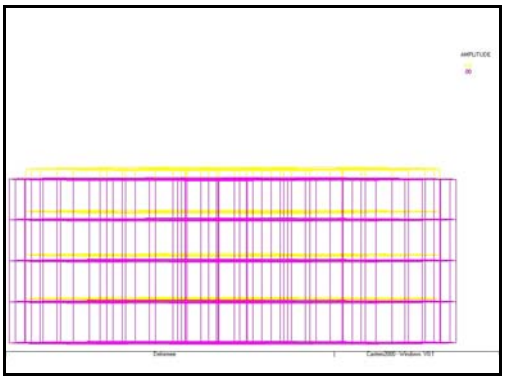

Figure 15: Deformation shape of the sample

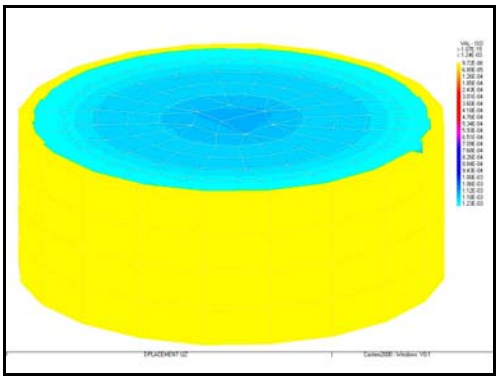

Figure 16: Variation of displacement UZ

Simulation of Free-swelling Tests by Alonso Model

For the simulation of the free swelling test, we used the Alonso model. The dimensions of the sample, the ring and the mesh previously used have been kept the same.

The deformed shape of the sample after swelling and the variation of displacement are given respectively in Figures 15 and 16.

Again, the results show very good convergence of theoretical and experimental values, since the error rates obtained for these simulations are less than 7% for the amplitude of swelling, while for the pressure, the error rates don't exceed 11% (Figure 17).

Examining the results of this simulation shows that the Alonso model can not simulate the response of very expansive soils (Figure 17 (a) and (c)), and that is because of the absence of load surface (SD Suction Decrease), the latter not being included in the model. Note that the version of software used (CASTEM 2000) is of the date 1998, while the third load surface was introduced in the Alonso model in 1999 (Version 1999).

CONCLUSIONS

Numerical analysis concerning the phenomenon of compressibility and swelling of soils by using Cam-Clay and Alonso models has been conducted. The latter, which is an approach for the estimation of swelling parameters, is well represented by the two models regarding the compressibility tests. Indeed, it was shown that the Cam-Clay model can not simulate the unloading phase of oedometric tests, therefore it can not simulate the swelling tests. This is because the model has only one load surface.

Unlikely, the Alonso model can simulate both phenomena even if it does not simulate correctly highly expansive soils. This is due to the absence of loading surface SD for the model used in the calculations.

In this work, a new approach for predicting swelling parameters has been proposed by numerical simulation. This approach has a great economic value because it allows to have an approximate idea about the impact of expansiveness of the soil on the distribution of stresses and strains within the sample and on the parameters of swelling.

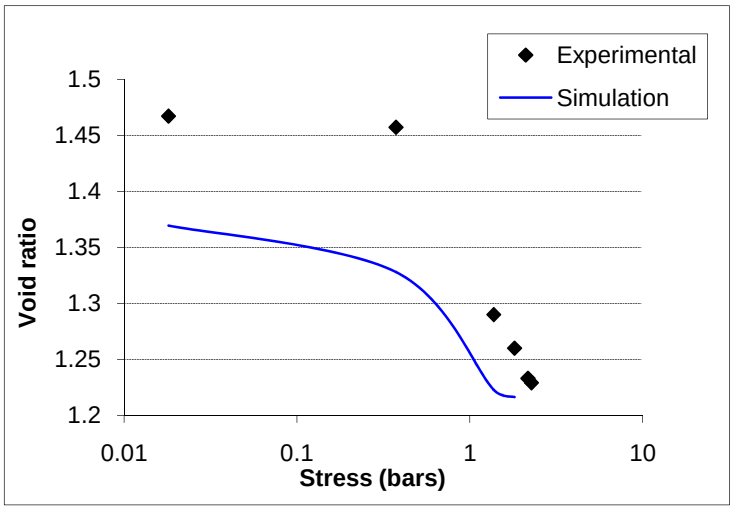

(a) Site: Bab El Assa, e_0 = 1.229

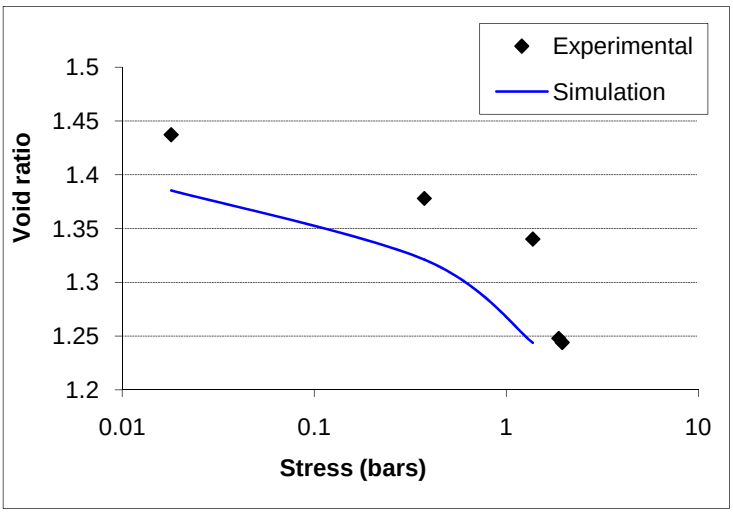

(b) Site: Bab El Assa, e_0 = 1.244

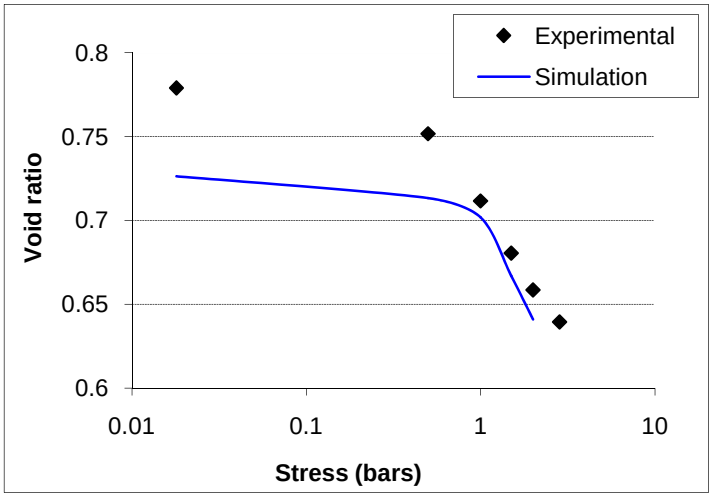

(c) Site: Ouled Mimoun, e_0 = 0.624

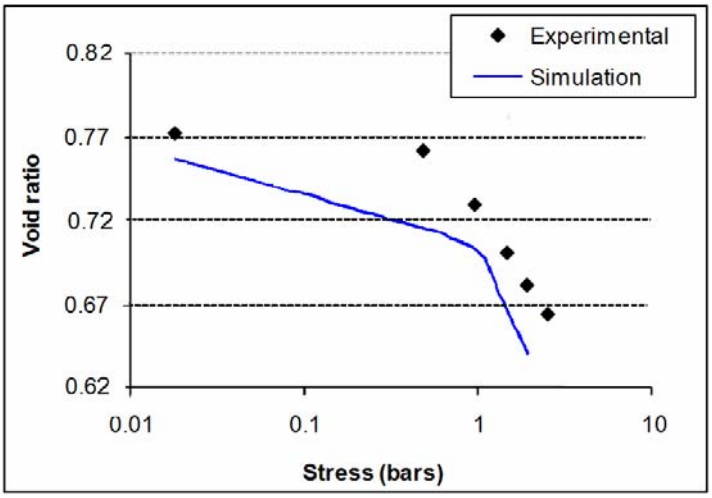

(d) Site: Ouled Mimoun, e_0 = 0.651

Figure 17: Simulation of free-swelling tests using the Alonso model

REFERENCES

Alonso, E. E., Gens, A. and Josa, A. 1990. A constitutive model for partially saturated soils, *Géotechnique,* 40 (3): 405-430.

Alonso, E. E., Gens, A. and Vaunat, J. 1999. Modelling the mechanical behavior of expansive clays, *Engineering Geology*, 54: 173-183.

Bekkouche, A. and Aissa Mamoune, S.M. 2005. Characteristics of Tlemcen's clay. *Electronic Journal of Geotechnical Engineering*, Volume 10C, Stillwater, OK 74075 (USA), ISSN 1089-3032.

Bekkouche, A., Djedid, A. and Aissa Mamoune, S.M. 2003. Identification et prévision des sols expansifs; 3ième Symposium International, Comportement des sols et des roches tendres, 22-24 Septembre 2003,

ISLYON‘ 03- ISBN 90-5809-604-1, Lyon.

Bekkouche, A., Djedid, A. and Aissa Mamoune, S.M. 2003. Modélisation numérique du comportement des argiles gonflantes par le modèle d’Alonso; Premier Congres International sur les Méthode Numériques Appliquées (CIMNA1), Beyrouth, Liban.

Callari, C., Auricchio, F. and Sacco, E. 1998. A finite-strain Cam-Clay model in the framework of multiplicative elasto-plasticity. *International Journal of Plasticity*, 14 (12): 1155-1187.

Djedid, A., Bekkouche, A. and Aissa Mamoune, S.M. 2001. Identification et prévision du gonflement de quelques sols de la région de Tlemcen (Algérie), *Bulletin des Laboratoires des Ponts et Chaussées*, N°233 de juillet-août 2001, 67-75.

Hujeux, J. C. 1985. Une loi de comportement pour le chargement cyclique des sols. Génie Parasismique, (V. Davidovici, Ed.), Presses de l’E.N.P.C., 287-302.

Karalis, T. K. 1990. Compressibilité des argiles gonflantes non saturées à partir des essais rhéologiques, *Can. Geotech. J.,* 67, Canada, 90-104.

Pakzad, M. 1995. Modélisation du comportement hydro-mécanique des argiles gonflantes à faible porosité, Thèse docteur, Orleans, France.

Robinet, J. C., Pakzad, M. and Plas, F. 1994. Un modèle rhéologique pour les argiles gonflantes, *Revue Française de Géotechnique*, 67, Paris, 57-67.